ACS APPLIED MATERIALS & INTERFACES

Research Article

www.acsami.org

Synthesis of (4-Hexyloxybenzoyl)butylsaure Methyl Amide/Poly(3-hexylthiophene) Heterojunction Nanowire Arrays

Nan Chen,[†,‡] Chao Liu,[†,‡] Jianhong Zhang,[†,‡] and Huibiao Liu*[,†]

[†]Beijing National Laboratory for Molecular Sciences (BNLMS), CAS Key Laboratory of Organic Solids, Institute of Chemistry, Chinese Academy of Sciences, Beijing 100190, P.R. China

[‡]Graduate University of Chinese Academy of Sciences, Beijing 100049, P.R. China

Supporting Information

ABSTRACT: Large-area P−N heterojunction organic semiconductor nanowire combined (4-hexyloxybenzoyl)butylsaure methyl amide (H-*t*-B) and Poly (3-hexylthiophene) (P3HT) were fabricated and the morphology and photoelectric properties were investigated by the growth of composition. The performance of light on/off switching of the H-*t*-B/P3HT heterojunction nanowire arrays was measured by the light irradiation on and off, the current in the devices showed two distinct states, the current was only 0.34 μA in the dark, while the current can reach 1.37 μA under the illumination of 45 mW/cm^2. The on/off switching ratio for the device of the heterojunction nanowire arrays is about 4.03.

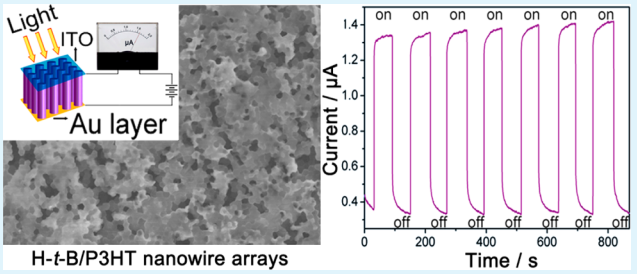

KEYWORDS: *large area heterojunction, blending organic semiconductor, template wetting, fullerene derivatives, nanowire arrays, light on/off switching*

INTRODUCTION

During the past 20 years, highly conjugated organic materials have been recognized as ideal candidates for use in next-generation electronic and optoelectronic devices because of their unique electrical, optical, and structural properties.[1−4] Interestingly, during these studies, researchers focused mainly on confirming new structures and properties, especially understanding the structure and size-based properties, which led to a new design principle for producing high-performance organic conjugated materials. In recent years, organic nanostructures chemistry has attracted more chemists to search the effective morphologies for these organic nanostructures of self-assembly. The rapid development of this new area of chemistry has promoted the understanding of the concepts of design and strategies of self-assembly of organic nanostructures. A lot of progress has been made in producing devices based on one-dimensional conducting polymers nanostructures and materials, both in the form of nanowire and nanotube[5−15] for applications on electronics,[16,17] photonics,[18,19] chemical sensors,[20−26] field emission devices,[27−35] solar cells,[36,37] and so on. The detailed morphology and orientation of these nanostructures are key parameters to determine their effectiveness in devices applications.[38,39] In particular, the design and synthesis (or fabrication) of vertically aligned nanowire arrays with controlled properties in devices are expected because of their well-defined channels for carriers.[40,41] Template-directed synthesis of one-dimensional conducting polymers nanostructures is widely used bottom-up synthetic strategy to control the dimensions of a variety of compositions of matter on length scales, and it is perhaps the most widely used subset of this strategy due to the large number of molecules that can be deposited by some easy methods.[42−47] Various methods of template have been developed to build both linear and branched conducting polymers nanostructures. Many new concepts for controlling synthesis heterojunction nanocomposites have been studied, such as metal−metal junctions, metal−polymer junctions, inorganic conducting polymers junctions, and inorganic−organic P−N junctions.[48] In fact, the physical and chemical properties of the independent component are much different after heterojunction composite formation. All carbon fullerene molecules have attracted the most attention and are expected to be widely applied to nanosciences and technology in recent years. However, how to combine carbon molecular materials and organic molecules for fabricating 1D P−N junctions to produce the uniformity of the size and shape on nanoscale with unique property is still a hot topic. The combined carbon and organic molecules are exploited for Enhanced optical, electrical and photoelectric conversion properties, due to increasing the surface area of P−N junction, reducing and preventing the compound of photogenerated excitons, and high efficiency of electric charge transfer by interpenetrating network structure.[49−51] In this article, we focused mostly on important qualitative features of new heterojunction nanowires between carbon materials and Poly (3-hexylthiophene) (P3HT), and adopted the use of synthetic new fullerene derivatives H-*t*-B with better solubility,

Received: June 27, 2012
Accepted: August 27, 2012
Published: August 27, 2012

so as to easily obtain density nanowire structure compared with the PCBM through template wetting method. Further, the approach aims to develop understanding of the properties of heterojunction materials between carbon and organic materials.

EXPERIMENTAL SECTION

A material is synthesized by template wetting[52] methods on nanoscale template within the vertically aligned pores. An efficient control is achieved on both diameter (by the pore diameter of the template) and length (by the amount of material supplied) by using this new strategy.

The AAO template was immersed in a solution of 0.2 mL of dichloromethane with 1 mg of fullerene derivative of (4-hexyloxybenzoyl)butylsaure methyl amide (H-*t*-B) and 1 mg P3HT, as shown in Figure 1 (To obtain the molecular structure of H-*t*-B, the

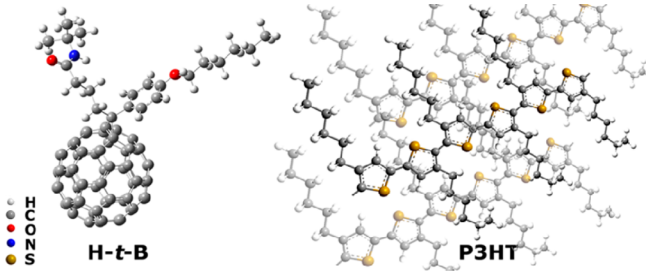

Figure 1. Molecular models of H-*t*-B and P3HT.

B3LYP/6-31tG* level using the Gaussian 03 program functional calculations were studied,[53] and P3HT molecule chain is a schematic diagram). The fullerene derivative is as the N-type materials in our experiment. The synthetic procedures of H-*t*-B were shown in the Supporting Information (Scheme S1). H-*t*-B/P3HT nanowires were controllably fabricated by evaporating the solvent at 40 °C for about 72 h. The alumina template was selectively etched by NaOH solution (2 M) with the assistance of an ultrasonic cleaning machine for characterization.

Materials. The synthesis of carbon materials H-*t*-B was shown in the Supporting Information; P3HT was purchased from Luminescence Technology Corp. All reagents were used as received. The anodic aluminum oxide (AAO) templates with porous diameter of about 200 nm (nominal) and a thickness of 60 μm were purchased from Whatman Corp.

Characterization. Field emission scanning electron microscopy (FESEM) images and energy-dispersive X-microanalysis spectrum (EDS) were taken from Hitachi S-4800 FESEM microscope at an accelerating voltage of 5 kV and 15 kV. Transmission electron microscopy (TEM) images and selective-area electron diffraction pattern (SAED) were taken from JEOL JEM-1011 microscope at an accelerating voltage of 100 kV. The micro morphology was tested by atomic force microscope (AFM) on SEIKO SPA400 ether, tapping mode (DFM). Conductivity of devices was recorded with a Keithley 4200 SCS at room temperature and a Micromanipulator 6150 probe station in a clean and shielded box at room temperature in air, as well as a Lakeshore XTPP6 low-temperature vacuum probe station.

RESULTS AND DISCUSSION

The nanostructures of heterojunction nanowire arrays were synthesized using N-type carbon materials H-*t*-B and P-type conducting polymers P3HT within anodic aluminum oxide (AAO) templates. Briefly, the AAO filter template was immersed in a solution of 0.2 mL of chlorobenzene with 1 mg of H-*t*-B and 1 mg P3HT. The solvent was evaporated within 72 h, and a solution of H-*t*-B and P3HT was gradually concentrated until the chlorobenzene complete evaporation. The resulting self-assembly in solution resulted in forming the bulk-heterojunction nanowires. Meanwhile, single-component nanowires of H-*t*-B and P3HT were also synthesized by the above process as comparative tests (SEM of single-component nanowires of H-*t*-B and P3HT were shown in the Supporting Information, Figure S1). Then the AAO template was coated with gold and used as the working electrode in the next electrical testing.

The EDS of H-*t*-B/P3HT heterojunction nanowires show that the compositions of the product were carbon oxygen, and sulfur, while the compositions of H-*t*-B nanowires and P3HT nanowires were carbon and oxygen, and carbon and Sulfur respectively, as shown in Figure S2 in the Supporting Information. Subsequently, we have calculated the components ratio by EDS analysis, which showed that the ratio of H-t-B and P3HT was about 7.4:10. The detailed microstructure and composition of a single nanowire were characterized by SEM, SAED, and TEM.

For the microstructures and compositions of H-*t*-B/P3HT nanowires, as-synthesized nanowires were characterized by SEM. The morphology and size of the H-*t*-B/P3HT heterojunction nanowire arrays are shown in the SEM images (Figure 2). Figure 2a shows the synthesis procedure of H-*t*-B/P3HT heterojunction nanowire arrays in AAO template, the as-synthesized H-*t*-B/P3HT heterojunction nanowire arrays looks "dark purple" as shown in Figure 2b (right), which was obviously different from the blank template as shown in Figure

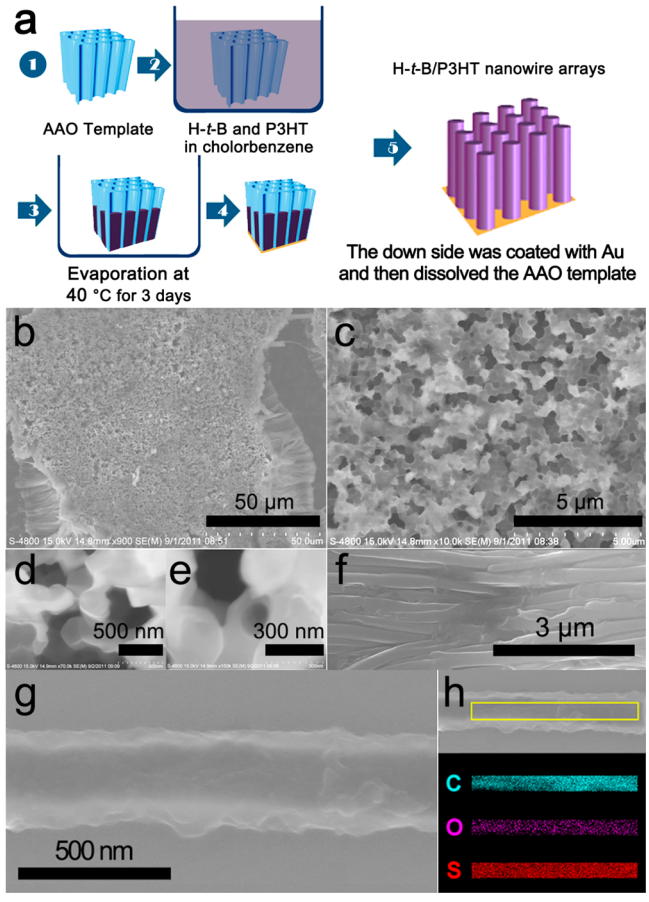

Figure 2. (a) Synthesis procedure of H-*t*-B/P3HT heterojunction nanowire arrays; (b–e) top view SEM image of H-*t*-B/P3HT heterojunction nanowire arrays under different magnification; (f, g) side view SEM images of H-*t*-B/P3HT heterojunction nanowire; (h) element mapping of single nanowire including C, O, and S element.

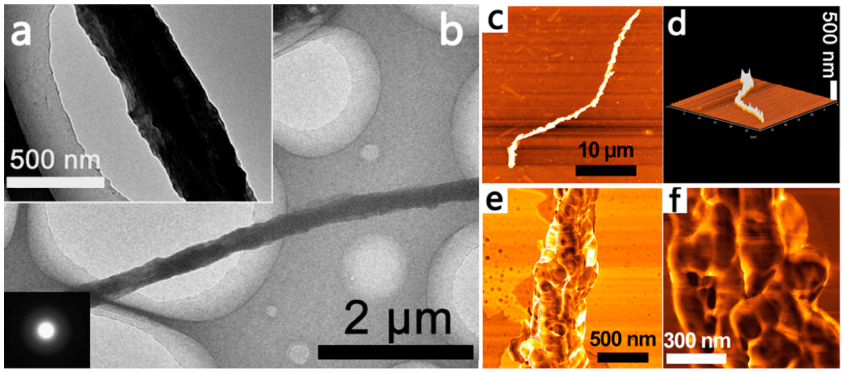

Figure 3. (a, b) TEM images of a single H-*t*-B/P3HT heterojunction nanowire under different magnifications, and SAED taken from segment in the nanowire (inset of the figure); (c) height image of a single H-*t*-B/P3HT heterojunction nanowire; (d) 3D height image of H-*t*-B/P3HT heterojunction nanowire; (e, f) phase image of H-*t*-B/P3HT heterojunction nanowire in different magnification.

2b (left). In images b and c in Figure 2, the large amount of nanowires indicated the high filling density of the membrane. These nanowires are well-defined, with a diameter of about 270 nm. Figure 2b depicted a large amount of nanowire arrays that were in the same length when the template was dissolved. Figure 2f shows the side view of H-*t*-B/P3HT heterojunction nanowire arrays. Furthermore, for TEM characterization, images a and b in Figure 3 clearly show the wirelike nanostructure with uniform diameter, and it had a typical amorphous SAED pattern, as illustrated by the inset in Figure 3b, which shows that the nanowire was amorphous. The micromorphology of H-*t*-B/P3HT heterojunction nanowire was tested by element mapping scanning on a substrate of silicon wafer. The O element was only existed in H-*t*-B, whereas S element existed only in P3HT, respectively. The element mapping images of Figure 2h show that the ingredients of H-*t*-B and P3HT are evenly mixed.

Micromorphology of H-*t*-B/P3HT heterojunction nanowire was measured by AFM. Height images were consistent with SEM results with same height and width (Figure 3c, d) in tapping mode on a substrate of silicon wafer. Images e and f in Figure 3 are phase images that showed there was phase separation of H-*t*-B and P3HT in the nanowire about 100 nm. The structure match of individual nanowires of H-*t*-B and P3HT is facilely creating homogeneous 1D H-*t*-B/P3HT P−N junction nanowires.

The electrical properties of H-*t*-B/P3HT heterojunction nanowire arrays were investigated by measurements of the current (I) versus time (T) and current (I) versus wavelength (λ). The devices were fabricated as described inset of the *I*-*V* curve graph in Figure 4a (right). The typical $I-T$ curves of the independent H-*t*-B nanowire arrays shows semiconductor property with a conductivity of about 1.25×10^{-7} S/m in the dark (Figure S3a, see Supporting Information) and the light on/off switching properties was not obvious. The $I-T$ curves of independent P3HT nanowire arrays show that the conductivity of 1×10^{-6} S/m in the dark, while the conductivity, which can increase to about 1.12×10^{-6} S/m with the increase illumination intensity (Figure S3b, see the Supporting Information). Figure 4a shows the on/off switching of H-*t*-B/P3HT heterojunction nanowire arrays under the illumination of 45 mW/cm^2 which was turned on and off repeatedly for several cycles. The current was monitored at bias of 5 V. With the light irradiation on and off, the current in the devices showed two distinct states, a "low" current in the dark and a "high" current under the illumination. In the dark, the current was only 0.34

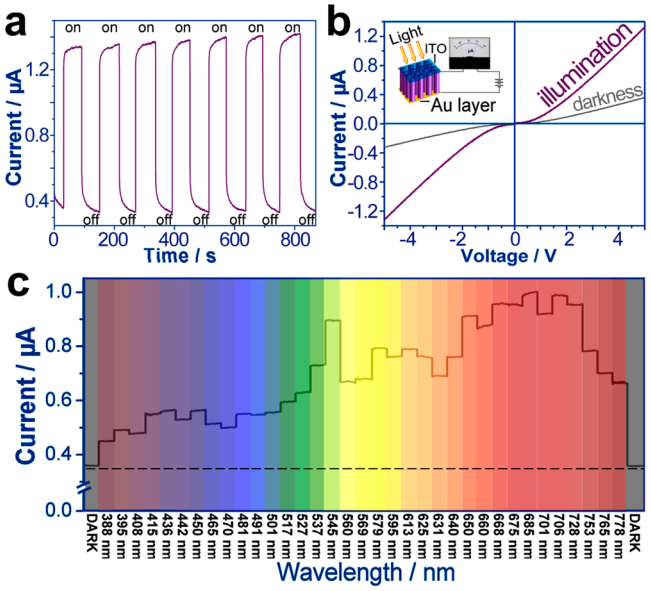

Figure 4. (a) On/off switching of H-*t*-B/P3HT heterojunction nanowire arrays upon pulsed illumination from full color with a power density of 45 mW/cm^2; (b) the conductivity of H-*t*-B/P3HT heterojunction nanowire arrays under illumination from full color with a power density of 45 mW/cm^2 and dark; (c) the conductivity of H-*t*-B/P3HT heterojunction nanowire arrays under different wavelengths of visible light.

μA while under the illumination of 45 mW/cm^2 the current reached 1.37 μA, which indicated an on/off switching ratio of 4.03. When the light was removed, the current was decreased to the initial value in an instant. The switching in the two states reveals that the response of H-*t*-B/P3HT is very sensitive and fast under illumination. Interestingly, heterojunction nanowire arrays shows excellent stability and repeatability for many cycle on/off switching.

For further investigation of illumination response, the H-*t*-B/P3HT heterojunction nanowire arrays were measured. The hetrojunction structure with good interface of P-type conducting polymers and N-type materials was expected to have unusual properties for new effects. The measurement shows an obvious enhancement of the conductivity of H-*t*-B/P3HT heterojunction nanowire arrays by hybrid excitations. The measurement of single P−N junction nanowire was also carried out. The results showed that the performance of electrons and holes transfer was strong in the single nanowire.

The electrons and holes can transport in the respective phase of the bulk heterojunction by light induced and be collected by the corresponding electrode, while the probability of the compound of photogenerated excitons was substantially reduced. The large area heterojunction nanowire arrays under the incident light with the appropriate energy can generate a large number of electrons and holes, These light-generated carriers was separated quickly under the electric field in the P−N junctions. Electrons diffused to the N-type H-*t*-B, whereas holes diffused to the P-type P3HT in the applied electric field, and transferred to the two electrodes respectively to generate a photocurrent, so the device of H-*t*-B/P3HT heterojunction nanowire arrays showed a high current density under the illumination compared with the darkness condition. On the other hand, the single-component nanowires (P3HT and H-*t*-B nanowire) produced hole or exciton cannot be effectively transmitted to the electrodes on both sides resulting in very weak effect of light on/off ratio, because the recombination of the exciton for the lack of P−N junctions in the heterojunction nanowire.

We have also studied the response of H-*t*-B/P3HT heterojunction nanowire arrays on different wavelengths of visible light region, Figure 4b shows the typical $I-\lambda$ curves obtained when H-*t*-B/P3HT heterojunction nanowire arrays are exposed to light with different wavelengths (the interval of wavelength is approximately 10 nm) after stabilization of current. Interestingly, under the illumination of different wavelengths of light, the conductivity of H-*t*-B/P3HT heterojunction nanowire arrays increased obviously compared with the dark situation. It can be seen that the current intensity of the H-*t*-B/P3HT heterojunction nanowire arrays is strongly increase at a region of about 700 nm of the wavelength of light, and the current intensity at other wavelengths of light was lower obviously than that of the region of 700 nm. The result indicates that the nanowire arrays exhibit high selectivity to wavelengths of light. The sensitivity of the photocurrent is obviously enhanced, due to the electron−hole pairs excited by the incident light with energy larger than the band gap, the energy level of H-*t*-B and P3HT were shown in Supporting Information, Figure S4; only light with enough photon energy is able to induce increase in conductance. The electron−hole pairs generated near the surface region typically have a lifetime shorter than those in the heterojunction; hence they contribute less to the photoconductance.[54] The slight increase of photosensitivity on the long wavelength of 650 nm is possibly due to the transition of carriers from defect states in the band gap to the conduction band.[55] The drop of sensitivity on the shorter wavelength side is attributed to the enhanced absorption of high-energy photons at or near the surface region of the semiconductor.[56]

In addition, we have measured the conductivity of the single nanowire containing numerous heterojunction (the nanodevice were depicted in the Supporting Information, Figure S5) under annealing temperature of 373 K, (taking into account the stable state of both H-*t*-B and P3HT, we chose the temperature. the TGA of H-*t*-B and P3HT ae shown in the Supporting Information, Figure S6). The advantage of annealing effect of the large area heterojunction nanowire arrays on conductivity is obvious. The sample of annealed at 373 K (Figure 5) showed the high conductivity while the on/off switching ratio of the sample did not change obviously compared with the unannealed sample (see the Supporting Information, Figure S7). The phenomenon may be due to a better contact on the interface between the two materials by annealing. The two components have been fully contact and mixing because the edges of two components become unclear after annealing at the temperature of 100 °C (see the Supporting Information, Figure S8). The result shows annealing can improve the interface contact between two different materials that is advantage formation of uniform contact interface for enlarge performance of heterojunction structure materials.

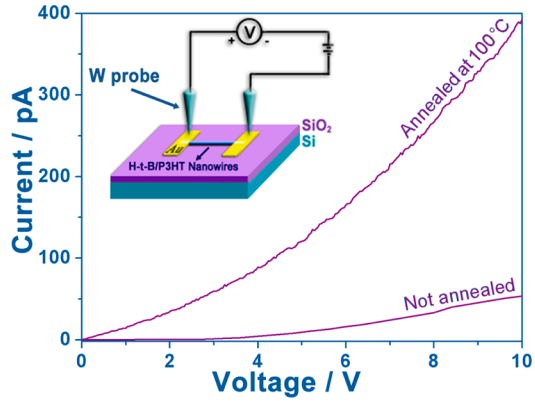

Figure 5. Typical current−voltage ($I-V$) curves for a single H-*t*-B/P3HT large area heterojunction nanowire under light illumination at room temperature for annealing temperature of 373 K and not annealed. The model nanodevice of single H-*t*-B/P3HT large area heterojunction nanowire was shown in the inset of this figure.

CONCLUSIONS

We have succeeded in producing highly ordered heterojunction nanowire arrays of H-*t*-B/P3HT which combined carbon molecular materials and organic molecules. The resulting 1D P−N junctions materials show the uniformity of the size and shape on nanoscale with unique property. The hetrojunction structure of P-type conducting polymers and N-type materials with good interface shows an obvious enhancement of the conductivity by hybrid excitations.The switching in the two states reveals that the response of H-*t*-B/P3HT is very sensitivity and fast under illumination. Interestingly, heterojunction nanowire arrays shows excellent stability and repeatability for many cycles on/off switching. The light on/off switching performance of H-*t*-B/P3HT large area heterojunction nanowire arrays is essential to determine the physical properties of optoelectronic materials for their applications.

ASSOCIATED CONTENT

Supporting Information

Synthesis and characterization route of (4-hexyloxybenzoyl)-butylsaure methyl amide (H-*t*-B); synthesis of H-*t*-B nanowire arrays and P3HT nanowire arrays; on/off switching of H-*t*-B and P3HT nanowire arrays; TGA of H-*t*-B and P3HT; the nanodevice of single H-*t*-B/P3HT nanowire images and conductivity properties. This information is available free of charge via the Internet at http://pubs.acs.org/.

AUTHOR INFORMATION

Corresponding Author

*E-mail: liuhb@iccas.ac.cn.

Notes

The authors declare no competing financial interest.

■ ACKNOWLEDGMENTS

This work was supported by the National Nature Science Foundation of China (21031006, 20873155, and 20831160507), and the National Basic Research 973 Program of China (2011CB932302 and 2012CD932900).

■ REFERENCES

(1) Barnes, W. L.; Samuel, I. D. W. *Science* **1999**, 211−212.
(2) Rogers, J. A.; Lagally, M. G.; Nuzzo, R. G. *Nature* **2011**, *477*, 45−53.
(3) Erb, T.; Zhokhavets, U.; Gobsch, G.; Raleva, S.; Stühn, B.; Schilinsky, P.; Waldauf, C.; Brabec, C. J. *Adv. Funct. Mater.* **2005**, *15*, 1193−1196.
(4) Zhang, L.; Qian, X. M.; Liu, L. B.; Shi, Z. Q.; Li, Y. J.; Wang, S.; Liu, H. B.; Li, Y. L. *Chem. Commun.* **2012**, *48*, 6166−6168.
(5) Liu, H. B.; Xu, J. L.; Li, Y. J.; Li, Y. L. *Acc. Chem. Res.* **2010**, *43*, 1496−1508.
(6) Teo, B. K.; Sun, X. H. *Chem. Rev.* **2007**, *107*, 1454−1532.
(7) Zheng, H. Y.; Li, Y. J.; Liu, H. B.; Yin, X. D.; Li, Y. L. *Chem. Soc. Rev.* **2011**, *40*, 4506−4524.
(8) Shankar, K.; Feng, X. J.; Grimes, C. A. *ACS Nano* **2009**, *3*, 788−794.
(9) Chen, N.; Huang, C. S.; Yang, W. L.; Chen, S. H.; Liu, H. B.; Li, Y. J.; Li, Y. L. *J. Phys. Chem. C* **2010**, *114*, 12982−12986.
(10) Jiang, X. C.; Tian, B. Z.; Xiang, J.; Qian, F.; Zheng, G. F.; Wang, H. T.; Mai, L. Q.; Lieber, C. M. *Proc. Natl. Acad. Sci. U.S.A.* **2011**, *108*, 12212−12216.
(11) Chen, N.; Qian, X. M.; Lin, H. W.; Liu, H. B.; Li, Y. J.; Li, Y. L. *Dalton Trans.* **2011**, *40*, 10804−10808.
(12) Liu, H. B.; Li, Y. L.; Xiao, S. Q.; Gan, H. Y.; Jiu, T. G.; Li, H. M.; Jiang, L.; Zhu, D. B.; Yu, D. P.; Xiang, B.; Chen, Y. F. *J. Am. Chem. Soc.* **2003**, *125*, 10794−10795.
(13) Lin, H. W.; Liu, H. B.; Qian, X. M.; Lai, S. W.; Li, Y. J.; Chen, N.; Ouyang, C. B.; Che, C. M.; Li, Y. L. *Inorg. Chem.* **2011**, *50*, 7749−7753.
(14) Ouyang, C. B.; Guo, Y. B.; Liu, H. B.; Zhao, Y. J.; Li, G. X.; Li, Y. J.; Song, Y. L.; Li., Y. L. *J. Phys. Chem. C* **2009**, *113*, 7044−7051.
(15) Cui, S.; Liu, H. B.; Gan, L. B.; Li, Y. L.; Zhu, D. B. *Adv. Mater.* **2008**, *20*, 2918−2925.
(16) Baik, J. M.; Zielke, M.; Kim, M. H.; Turner, K. L.; Wodtke, A. M.; Moskovits, M. *ACS Nano* **2010**, *4*, 3117−3122.
(17) Okawa, Y.; Mandal, S. K.; Hu, C. P.; Tateyama, Y.; Goedecker, S.; Tsukamoto, S.; Hasegawa, T.; Gimzewski, J. K.; Aono, M. *J. Am. Chem. Soc.* **2011**, *133*, 8227−8233.
(18) Barrelet, C. J.; Greytak, A. B.; Lieber, C. M. *Nano Lett.* **2004**, *4*, 1981−1985.
(19) Yan, R. X.; Pausauskie, Pe.; Huang, J. X.; Yang, P. D. *PNA* **2009**, *106*, 21045−21050.
(20) Rogers, J. A.; Lagally, M. G.; Nuzzo, R. G. *Nature* **2011**, 45−53.
(21) Zhong, Z. H.; Wang, D. L.; Cui, Y.; Bockrath, M. W.; Lieber, C. M. *Science* **2003**, 1377−1379.
(22) Engel, Y.; Elnathan, R.; Pevzner, A.; Davidi, G.; Flaxer, E.; Patolsky, F. *Angew. Chem., Int. Ed.* **2010**, *49*, 6830−6835.
(23) Dang, X. N.; Yi, H.; Ham, M. H.; Qi, J. F.; Yun, D. S.; Ladewski, R.; Strano, M. S.; Hammond, P. T.; Belcher, A. M. *Nat. Nanotechnol.* **2011**, *6*, 377−384.
(24) Chen, P. C.; Sukcharoenchoke, S.; Ryu, K.; Gomez de Arco, L.; Badmaev, A.; Wang, C.; Zhou, C. W. *Adv. Mater.* **2010**, *22*, 1900−1904.
(25) Zhao, Y. S.; Wu, J. S.; Huang, J. X. *J. Am. Chem. Soc.* **2009**, *131*, 3158−3159.
(26) Jang, J.; Bae, J.; Park, E. *Adv. Funct. Mater.* **2006**, *16*, 1400−1406.
(27) Gan, H. Y.; Liu, H. B.; Li, Y. J.; Zhao, Q.; Li, Y. L.; Wang, S.; Jiu, T. G.; Wang, N.; He, X. R.; Yu, D. P.; Zhu, D. B. *J. Am. Chem. Soc.* **2005**, *127*, 12452−12453.
(28) Ouyang, C. B.; Guo, Y. B.; Liu, H. B.; Zhao, Y. J.; Li, G. X.; Li, Y. J.; Song, Y. L.; Li, Y. L. *J. Phys. Chem. C* **2009**, *113*, 7044−7051.
(29) Liu, H. B.; Liu, Z.; Qian, X. M.; Guo, Y. B.; Cui, S.; Sun, L. F.; Song, Y. L.; Li, Y. L.; Zhu, D. B. *Cryst. Growth Des.* **2010**, *10*, 237−243.
(30) Liu, H. B.; Zhao, Q.; Li, Y. L.; Liu, Y.; Lu, F. S.; Zhuang, J. P.; Wang, S.; Jiang, L.; Zhu, D. B.; Yu, D. P.; Chi, L. F. *J. Am. Chem. Soc.* **2005**, *127*, 1120−1121.
(31) Chen, N.; Qian, X. M.; Lin, H. W.; Liu, H. B.; Li, Y. L. *J. Mater. Chem.* **2012**, *22*, 11068−11072.
(32) Liu, H. B.; Zuo, Z. C.; Guo, Y. B.; Li, Y. J.; Li, Y. L. *Angew. Chem., Int. Ed.* **2010**, *49*, 2705−2707.
(33) Cui, S.; Li, Y. L.; Guo, Y. B.; Liu, H. B.; Song, Y. L.; Xu, J. L.; Lv, J.; Zhu, M.; Zhu, D. B. *Adv. Mater.* **2008**, *20*, 309−313.
(34) Huang, C. S.; Wen, L. P.; Liu, H. B.; Li, Y. L.; Liu, X. F.; Yuan, M. J.; Zhai, J.; Jiang, L.; Zhu, D. B. *Adv. Mater.* **2009**, *21*, 1721−1725.
(35) Huang, C. S.; Li, Y. L.; Song, Y. L.; Li, Y. J.; Liu, H. B.; Zhu, D. B. *Adv. Mater.* **2010**, *22*, 3532−3536.
(36) Guo, Y. B.; Zhang, Y. J.; Liu, H. B.; Lai, S. W.; Li, Y. L.; Li, Y. J.; Hu, W. P.; Wang, S.; Che, C. M.; Zhu, D. B. *J. Phys. Chem. Lett.* **2010**, *1*, 327−330.
(37) Xu, C.; Wang, X. D.; Wang, Z. L. *J. Am. Chem. Soc.* **2009**, *131*, 5866−5872.
(38) Shen, X. J.; Sun, B. Q.; Yan, F.; Zhao, J.; Zhang, F. T.; Wang, S. D.; Zhu, X. L.; Lee, S. −T. *ACS Nano* **2010**, *4*, 5869−5876.
(39) Shen, X. J.; Sun, B. Q.; Liu, D.; Lee, S. −T. *J. Am. Chem. Soc.* **2011**, *133*, 19408−19415.
(40) Prieto, A. L.; Sander, M. S.; Martin−Gonzalez, M. S.; Gronsky, R.; Sands, T.; Stacy, A. M. *J. Am. Chem. Soc.* **2001**, *123*, 7160−7161.
(41) Yin, A. J.; Li, J.; Jian, W.; Bennett, A. J.; Xu, J. M. *Appl. Phys. Lett.* **2001**, *79*, 1039−1041.
(42) Liu, H. B.; Cui, S.; Guo, Y. B; Li, Y. L.; Huang, C. S.; Zuo, Z. C.; Yin, X. D.; Song, Y. L.; Zhu, D. B. *J. Mater. Chem.* **2009**, *19*, 1031−1036.
(43) Ouyang, C. B.; Liu, H. B.; Qian, X. M.; Lin, H. W.; Chen, N.; Li, Y. L. *Dalton Trans.* **2011**, *40*, 3553−3557.
(44) Gan, H. Y.; Liu, H. B.; Li, Y. L.; Gan, L. B.; Jiang, L.; Jiu, T. G.; Wang, N.; He, X. R.; Zhu, D. B. *Carbon* **2005**, *43*, 205−208.
(45) Lin, H. W.; Liu, H. B.; Qian, X. M.; Ouyang, C. B.; Li, Y. L. *Dalton Trans.* **2011**, *40*, 4397−4401.
(46) Li, G. X.; Li, Y. L.; Qian, X. M.; Liu, H. B.; Lin, H. W.; Chen, N.; Li, Y. J. *J. Phys. Chem. C* **2011**, *115*, 2611−2615.
(47) Liu, H. B.; Li, Y. L.; Jiang, L.; Luo, H. Y.; Xiao, S. Q.; Fang, H. J.; Li, H. M.; Zhu, D. B.; Yu, D. P.; Xu, J.; Xiang, B. *J. Am. Chem. Soc.* **2002**, *124*, 13370−13371.
(48) Guo, Y. B.; Tang, Q. X.; Liu, H. B.; Zhang, Y. J.; Li, Y. L.; Hu, W. P.; Wang, S.; Zhu, D. B. *J. Am. Chem. Soc.* **2008**, *130*, 9198−9199.
(49) Ren, G. Q.; Wu, P. T.; Jenekhe, S. A. *ACS Nano* **2011**, *5*, 376−384.
(50) Mawyin, J.; Shupyk, I.; Wang, M. Q.; Poize, G.; Atienzar, P.; Ishwara, T.; Durrant, J. R.; Nelson, J.; Kanehira, D.; Yoshimoto, N.; Martini, C.; Shilova, E.; Secondo, P.; Brisset, H.; Fages, F.; Ackermann, J. *J. Phys. Chem. C* **2011**, *115*, 10881−10888.
(51) Kim, F. S.; Ren, G. Q.; Jenekhe, S. A. *Chem. Mater.* **2011**, *23*, 682−732.
(52) Steinhart, M.; Wendorff, J. H.; Greiner, A.; Wehrspohn, R. B.; Nielsch, K.; Schilling, J.; Choi, J.; Goesele, U. *Science* **2002**, *296*, 1997.
(53) Wu, D.; Paddison, S. J.; Elliott, J. A. *Macromolecules* **2009**, *42*, 3358−3367.
(54) Jie, J. S.; Zhang, W. J.; Jiang, Y.; Meng, X. M.; Li, Y. Q.; Lee, S. T. *Nano Lett.* **2006**, *6*, 1887−1892.
(55) Fan, Z.; Chang, P. C.; Lu, J. G.; Walter, E. C.; Penner, R. M.; Lin, C. H.; Lee, H. P. *Appl. Phys. Lett.* **2004**, *85*, 6128−6130.
(56) Amalnerkar, D. P. *Mater. Chem. Phys.* **1999**, *60*, 1−21.